DEVELOPMENTAL BIOLOGY **199,** 150–163 (1998)
ARTICLE NO. DB988914

# The Transition to Endoreduplication in Trophoblast Giant Cells Is Regulated by the mSNA Zinc Finger Transcription Factor

**Hiroki Nakayama,*,[1] Ian C. Scott,*,†,[1] and James C. Cross*,†,‡,[1,2]**

**Program in Development and Fetal Health, Samuel Lunenfeld Research Institute, Mount Sinai Hospital, 600 University Avenue, Toronto, Ontario M5G 1X5 Canada; and †Department of Medical Genetics and Microbiology and ‡Department of Obstetrics and Gynaecology, University of Toronto, Toronto, Ontario M5G 1X5 Canada*

**Terminal cell differentiation is usually associated with cell cycle exit. In some lineages, however, cells undergo continued rounds of DNA synthesis without intervening mitoses (endoreduplication) resulting in polyploid nuclei. This is striking in rodent trophoblast giant cells which contain up to 1000N of DNA. In *Drosophila,* the *Escargot* gene has been implicated in regulating the transition from mitotic cell cycles to endocycles during development. We found that a murine homologue, *mSna,* was expressed in mouse trophoblast and was downregulated during giant cell differentiation. The mSNA zinc finger protein bound to E-box DNA elements and, in transfected C3H10T1/2 fibroblasts, acted as a transcriptional repressor. The maximal repressive effect was dependent on both the zinc finger DNA-binding domain and the N-terminal, seven-amino-acid SNAG domain. Misexpression experiments in Rcho-1 trophoblast cells revealed that *mSna* regulates the transition from replicating precursor cells to committed giant cells: overexpression blocked, whereas antisense RNA-mediated underexpression promoted trophoblast giant cell differentiation. Overexpression of *mSna* in precursor cells had no effect on cell cycle kinetics, but did increase cyclin A and B levels, implying actions during G2. These effects were dependent on both the zinc finger and SNAG domains. Together, these data suggest that mSNA has an ESCARGOT-like function to repress the transcription of genes that promote the transition from mitotic to endoreduplicative cell cycles in rodent trophoblast.** 

## INTRODUCTION

During the normal cell cycle, duplication of genomic DNA is systematically followed by mitosis resulting in two daughter cells with diploid DNA content, equivalent to the parent cell. The fidelity of this process is critical to the maintenance of the genome during embryonic development and particularly during passage through the germline. This mitotic cell cycle is orchestrated by regulators that function at distinct phases of the cycle (Hartwell and Kastan, 1994; Sherr, 1993). The primary regulators are cyclin/cyclin-dependent kinase (cdk) complexes whose activities fluctuate during the cell cycle. Distinct cyclin/cdk complexes are required at each step; cyclin E/cdk2 is essential for G1/S transition, whereas cyclin B/cdk1 is required for mitosis (Sherr, 1993). Progression through a complete cycle therefore depends on stereotypic activation and repression of cyclin/cdk activities, events that are usually closely coupled. For example, cyclin E/cdk2 is essential for activation of cyclin B/cdk1 later in the cell cycle (Guadagno and Newport, 1996). In turn, G2 cyclin activity diminishes the expression of G1 cyclins (Amon *et al.,* 1993). Consistent with this, mutations in fission yeast which interfere with activity of the cyclin B/cdk1 complex (e.g., cdc2/cdc13) are unable to complete mitosis, but significantly also undergo endoreduplication (Hayles *et al.,* 1994). Apart from this coupling mechanism, how cells maintain diploidy is not well understood. In mammals, p53 plays an important role since null mutations in the p53 gene lead to a tendency for cells to endoreduplicate (Cross *et al.,* 1995b). In the same way that p53 is activated following DNA damage, it is possible that p53 is also responsive to DNA content.

In rare examples in nature, cells re-replicate their DNA in the absence of a subsequent mitosis, a process called endoreduplication. It is a normal feature in trophoblast

[1] These authors contributed equally to this work.

[2] To whom correspondence should be addressed. Fax: (416) 586-8588. E-mail: cross@mshri.on.ca.

0012-1606/98 $25.00

giant cells of the rodent placenta, in mammalian hepatocytes and megakaryocytes, and in salivary glands and some larval cells in *Drosophila*. In trophoblast giant cells of the rodent placenta repeated endocycles may result in cells with up to 1000 haploid genome (1000N) DNA content (Zybina and Zybina, 1985) in which the DNA exists in a polytene arrangement (Varmuza *et al.*, 1988). The biological functions of endoreduplication in trophoblast remain a mystery and the factors that control the differentiation of trophoblast cells have only just begun to be understood. Helix-loop-helix transcription factors encoded by *Hxt* and *Mash-2* appear to play an important role. *Mash-2* is essential for the maintenance of diploid trophoblast precursor cells and, in its absence, excess trophoblast giant cell differentiation occurs (Guillemot *et al.*, 1994). By contrast, *Hxt* appears to have the opposite activity in promoting giant cell differentiation (Cross *et al.*, 1995a; Riley *et al.*, 1998). In transfected Rcho-1 trophoblast cells, *Mash-2* and *Hxt* are each sufficient to either block or promote giant cell differentiation, respectively (Cross *et al.*, 1995a). However, at present it is unclear whether these effects are directly related to cell cycle events.

Recent work suggests that the *Escargot* gene functions to prevent endoreduplication in *Drosophila*. *Escargot* mutants show abnormal development in which imaginal disc cells that normally show replicative cell cycles undergo endoreduplication instead (Hayashi *et al.*, 1993). Conversely, ectopic expression of *Escargot* suppresses endoreduplication in the salivary glands (Fuse *et al.*, 1994). These data strongly suggest that *Escargot* is essential for the maintenance of cell diploidy in certain tissues. Cloning of the *Escargot* gene showed that it was a member of the *Snail* family that encodes a zinc finger transcription factor (Hayashi *et al.*, 1993). The activity of *Escargot* in *Drosophila* suggested the possibility that an *Escargot*-like gene could regulate the transition from the mitotic cell cycle to the endocycle in the trophoblast lineage. Several genes related to *Escargot* and *Snail* have been identified in vertebrates and, within the zinc finger domain, the encoded proteins are highly conserved. The mouse *Sna* (*mSna*) gene was described by two groups who reported its expression in mesoderm and neural crest derivatives (Nieto *et al.*, 1992; Smith *et al.*, 1992). The *mSna* sequence is similar to both *Snail* and *Escargot* from *Drosophila*. The gene was given the name *mSna* due to the fact that its mesodermal expression pattern was reminiscent of that of Drosophila *Snail*. However, the gene was also found to be expressed in day 7.5 mouse trophoblast tissue (Nieto *et al.*, 1992; Smith *et al.*, 1992). We have confirmed this latter finding and show here that *mSna* expression is in fact restricted to trophoblast giant cell precursors and is shut off with their differentiation. We also present evidence that *mSna* inhibits giant cell differentiation, and therefore endoreduplication, in trophoblast. This activity is dependent on the sequence-specific DNA-binding and transcriptional repression activities of the mSNA protein. We conclude, therefore, that the function of *mSna* in rodent trophoblast appears similar to that of the *Escargot* gene in *Drosophila*.

## MATERIALS AND METHODS

***Plasmids.*** Expression vectors were constructed using standard molecular biology techniques (Sambrook *et al.*, 1989). pREP-mSna and pREP-antimSna, *mSna* sense and antisense expression vectors, were made by ligating the *Xho*I/*Bam*HI fragment from the *mSna* clone 5-15 (Smith *et al.*, 1992) into pREP7 and pREP10 (Invitrogen), respectively. pREP-mSnaΔSNAG, a mammalian expression vector encoding a SNAG domain-deleted version of mSNA, lacking the first seven amino acids, was generated from clone 5-15 by PCR using the primers JCC189 (5′-CGGAATTC**ATG**AGGAAGCCGTCCGACCCC-3′) and JCC190 (5′-TCGGATGTGCATCTTCAGAGCGCC-3′). An *Eco*RI/*Bgl*II fragment of the PCR product was ligated into pBS-mSna (*Eco*RI/*Hin*dIII fragment from clone 5-15 in pBluescript-SK+), creating pBS-mSnaΔSNAG. The *Sma*I/*Hin*dIII fragment from pBS-mSnaΔSNAG was then ligated into the *Pvu*II and *Hin*dIII sites of pREP7. pREP-VP16mSna, encoding an N-terminal fusion of the VP16 acidic activation domain to mSNAΔSNAG, was made by first ligating a *Bam*HI/*Eco*RI insert containing the VP16 acidic activation domain into pBS-mSnaΔSNAG to generate pBS-VP16mSna. The *Hin*dIII fragment from pBS-VP16mSna was then ligated into pREP7. pEF-mtmSna, a mammalian expression vector encoding a myc-tagged full-length mSNA protein, was generated by ligating the *Eco*RI fragment from clone 5-15 into pEFmPLINK (Marais *et al.*, 1995). pEF-mtmSnaΔZF, encoding myc-tagged mSNA lacking the zinc finger domain, was constructed by first ligating an *Eco*RI/*Bgl*II fragment of clone 5-15 into pBluescript-SK+. The *Eco*RI/*Xba*I insert from this plasmid was subsequently ligated into pEFmPLINK. pREP-dSna and pREP-dEsg, Drosophila *Snail* and *Escargot* mammalian expression vectors, were constructed by cloning the *Not*I/*Kpn*I fragments of the *Snail* and *Escargot* cDNAs into pREP10. The vectors pβActin-LacZ, pCMV-Mash-2 (Cross *et al.*, 1995a), pCMV-ME2 (Chiaramello *et al.*, 1995), and p2E MCK-CAT and p2mE MCK-CAT (Johnson *et al.*, 1992) have been previously described. The T7 promoter *Escherichia coli* expression vector pHK was produced by ligating the annealed oligos JCC102 (5′-CTAGTGCAAGAAGAGCATCTGTGAAG-3′) and JCC103 (5′-GATCCTTCACAGATGCTCTTCTTGCA-3′) between the *Nhe*I and *Bam*HI sites of pRSETB (Invitrogen). pHK-mSna, an N-terminal truncated mSNA bacterial expression vector, was generated by first ligating the *Pst*I/*Bam*HI fragment from clone 5-15 into pBluescript-SK(+). The *Eco*RI digestion product was then ligated into pHK. pHis-Mash-2, an *E. coli* expression vector encoding rat MASH-2, was generated by ligating the *Hin*dIII fragment of pRatprMash-2 (Johnson *et al.*, 1990) into pRSETA (Invitrogen). pT7-N3, encoding Syrian hamster E47, has been previously described (Blanar and Rutter, 1992).

***In situ hybridization.*** Day 8.5 and 10.5 murine conceptuses were fixed in decidua with 4% paraformaldehyde. The tissues were embedded in paraffin, sectioned, and subjected to RNA *in situ* hybridization as previously described (Millen and Hui, 1996). Antisense $^{33}$P-labeled riboprobes were prepared using an RNA transcription kit (Stratagene). Probes specific to *mSna* (Smith *et al.*, 1992), *Mash-2* (Guillemot *et al.*, 1994), and *PL-I* (Jackson *et al.*, 1986) have been previously described. Sections were incubated in hybridization buffer containing $1 \times 10^5$ cpm/$\mu$l of riboprobe.

***Electrophoretic mobility shift assays.*** *In vitro* transcription/translation of *E47, mSna,* and *Mash-2* was performed using the

Promega $T_NT$ rabbit reticulolysate kit and the plasmids pT7-N3, pHK-mSna, and pHis-Mash-2, according to manufacturer's instructions. Electrophoretic mobility shift assays were carried out as previously described (Fuse *et al.,* 1994) using the control (no DNA template) *in vitro* transcription/translation product to balance the amount of lysate added to each lane. Proteins were preincubated for 15 min at 30°C prior to the addition of 10,000 cpm (1000 cpm for protein:protein competition assays) of $^{32}$P-labeled probe. Binding reactions were carried out for 15 min at room temperature, followed by resolution of complexes via electrophoresis in 5% nondenaturing acrylamide gels (run at 7 V/cm). For competition experiments a 200-fold excess of unlabeled oligonucleotide was added prior to the preincubation step. Probes were labeled by fill-in reactions using [$\alpha$-$^{32}$P]dCTP and Klenow polymerase (Sambrook *et al.,* 1989). Annealed double-stranded oligonucleotides, corresponding to regions of the muscle creatine kinase (MCK) (Johnson *et al.,* 1992) and *PL-I* (Ng *et al.,* 1994) promoters, as well as various E- and N-box sequences (shown in bold), were as follows: MCK E-box (5′-GATCCCCCCAA**CACCTG**CTGCCTGA-3′, 5′-GATCTCAGGCAGCAGGTGTTGGGGG-3′); HIV LTR NF-κB site (5′-GATCCTAGAGGGGACTTTCCAGAGGGGATTTCCTGCAGT-3′, 5′- GATCCACTGCAGGAAATCCCCTCTGGAAAGTCCCCTCTA-3′); PL-I E-box(a) (5′- GATCTCCAGAT**CACATG**GGG-3′, 5′-GATCCCCCATGTGATCTGGA-3′); PL-I E-box(b) (5′-AATTCAGTC**CAGATG**ATCCG-3′, 5′-GATCCGGATCATCTGGACTG-3′); Th1 E-box (5′-GATCCATTG**CATCTG**GATTCCAGA-3′, 5′-GATCTCTGGAATCCAGATGCAATG-3′); E(Spl) N-box (5′- GATCCACGC**CACGAG**C**CACAAG**GATTA-3′, 5′-GATCTAATCCTTGTGGCTCGTGGCGTG-3′); and AP4 E-box (5′-GATC CAACAG**CAGCTG**CAGTG-3′, 5′-GATCCACTGCAGCTGCTGTTG-3′).

***Cell culture and transfection.*** C3H10T1/2 and NIH/3T3 fibroblasts were cultured in Dulbecco's modified Eagle medium containing 10% fetal bovine serum (Hyclone) plus 50 $\mu$M $\beta$-mercaptoethanol, penicillin (100 U/ml), and streptomycin (100 $\mu$g/ml) (Gibco BRL). Rcho-1 cells were maintained in NCTC-135 medium containing 20% fetal bovine serum, 50 $\mu$M $\beta$-mercaptoethanol, 1 mM Pyruvate, penicillin (100 U/ml), and streptomycin (100 $\mu$g/ml) as previously described (Faria and Soares, 1991). For the isolation of homogeneous undifferentiated Rcho-1 stem cell subpopulations, trypsin-labile cells were collected after brief trypsinization (0.25% trypsin, 2 min) from a semiconfluent culture dish, diluted 1:6, and replated.

Transient DNA transfections using lipofectamine were carried out according to manufacturer's instructions (Gibco BRL). C3H10T1/2 cells were plated at a density of $1 \times 10^5$ cells per 35-mm dish 24 h prior to addition of complexes containing 5 $\mu$l of lipofectamine and 2 $\mu$g of DNA (100 ng of p$\beta$Actin-LacZ, 800 ng of p2E or 2mE MCK-CAT, and the indicated amount of expression vector). Fresh medium was added 24 h posttransfection, and cells were harvested after an additional 24 h. Chloramphenicol acetyltransferase levels were measured using a CAT ELISA kit (Boehringer-Mannheim) and were normalized to $\beta$-galactosidase activity (Sambrook *et al.,* 1989). Values are reported relative to CAT levels measured for empty pREP7 alone and represent means ± SE for duplicate transfected dishes in each experiment.

Transient transfections of Rcho-1 stem cells were performed 5 h after replating to 35-mm dishes. For differentiation assays, cells were cotransfected with 0.5–1.0 $\mu$g of the indicated *mSna* or empty expression vector and 0.1–0.2 $\mu$g of p$\beta$Actin-LacZ. The cells were fixed 48 h posttransfection and stained for $\beta$-galactosidase activity (Sambrook *et al.,* 1989). The proportion of $\beta$-galactosidase-positive cells which had differentiated to trophoblast giant cells was scored based on cellular morphology as previously described (Cross *et al.,* 1995a). For proliferation assays Rcho-1 stem cells were split at a low (1:10) density 5 h prior to transfection with control or antisense *mSna* expression vector and p$\beta$Actin-LacZ. Cells were stained for $\beta$-galactosidase activity 48 h posttransfection. The number of clusters of blue-staining cells, each assumed to have arisen from proliferation of a single transfected cell, was counted. Stable Rcho-1 transfectants were obtained via lipofectamine-mediated transfection with the indicated expression vector, followed by selection with hygromycin B (80 $\mu$g/ml, Sigma) 48 h posttransfection. Ten clones were isolated and analyzed for each vector.

***Northern blot hybridization.*** RNA was extracted and analyzed as described previously (Nakayama *et al.,* 1997). Probes for *mSna* (Smith *et al.,* 1992), *cyclin A2* (Sweeney *et al.,* 1996), *cyclin B1* (Chapman and Wolgemuth, 1992), and *GAPDH* (Fort *et al.,* 1985) have been described previously. Membranes were exposed to phosphor screens. Intensity of the signals was quantified using the Image Quant program of the Storm 860 system (Molecular Dynamics).

***Cell cycle kinetics.*** Cell cycle length was estimated from the cell doubling time: this was calculated from counts of cell numbers in eight microscopic fields at 2, 24, and 48 h after replating at a 1:10 dilution. To estimate cell cycle phase lengths, Rcho-1 stem cells were plated on coverslips and pulse-labeled with [$^3$H]thymidine (1 $\mu$Ci/ml) for 1 h. After labeling, the medium was replaced and cells were fixed with 4% paraformaldehyde at 1-h intervals for 12 h. Fixed specimens were covered with emulsion and subjected to autoradiography (Millen and Hui, 1996) to detect [$^3$H]thymidine incorporation. The proportion of cells with silver grains within the nucleus was determined via light microscopy. S-phase length was calculated as the product of the total cell cycle length and the proportion of labeled cells at $t = 0$ h. The length of G2 was estimated as the time taken after the pulse for silver grains to appear in the M-phase cells. M-phase length was calculated as the product of the total cell cycle length and the proportion of cells displaying mitotic figures. G1 length was estimated from the above values (G1 = total cell cycle length − S − G2 − M).

***Immunolocalization of myc-tagged mSNA.*** Cells were grown on coverslips for 2 days after transfection with pEF-mtmSna or pEF-mtmSnaΔZF. Cells were fixed with 4% paraformaldehyde and incubated for 1 h with undiluted supernatant from the 9E10 anti-human c-myc hybridoma (ATCC CRL-1729) (Evan *et al.,* 1985). Following washing steps, a 1:100 dilution of an anti-mouse IgG–FITC conjugate (Sigma) secondary antibody was subsequently applied for 1 h. After immunostaining, DNA was stained with bisbenzimide (Sigma) for 2 min. Cells were analyzed using fluorescence microscopy.

***3T3 cell synchronization and analysis.*** 3T3 cell cycle synchronization at the G1 phase was performed by serum starvation (0.5% FBS) for 3 days. After serum addition (final 10%), cells were lysed in denaturing solution for RNA extraction every 2 h from time 0 to 24 h. Cells on coverslips were pulse-labeled with [$^3$H]thymidine (1 $\mu$Ci/ml) for 2 h at different times following serum addition, fixed, and subjected to autoradiography as described above. The proportions of labeled (S-phase) cells and cells demonstrating mitotic figures (M-phase) were counted. The effects of cycloheximide on *mSna* mRNA levels were assayed by the addition of 10 $\mu$g/ml cycloheximide (Sigma) to synchronized cells upon serum addition. RNA was collected at 0, 0.25, 0.5, 1, 2, 4, 6, 8, and 10 h and subjected to Northern blot analysis as described above.

***Quantitation of nuclear DNA content.*** Proliferating Rcho-1 and HeLa cells were trypsinized briefly, fixed in ethanol, and

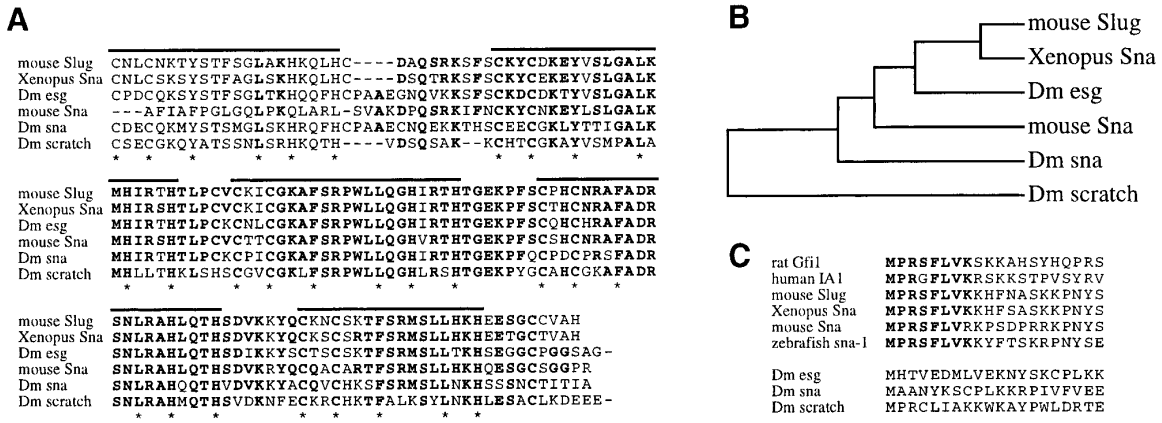


**FIG. 1.** Evolution of SNAIL-related proteins. (A) Alignment of the zinc finger regions of *Mus musculus* (mouse) SLUG (U79550), *Xenopus laevis* SNA (X53450), *Drosophila melanogaster* ESCARGOT (M83207), *M. musculus* SNA (X67253; M95604), *D. melanogaster* SNAIL (Y00288), and *D. melanogaster* SCRATCH (U36477) proteins. Bold indicates amino acid identity compared with mSNA. Gaps have been introduced in order to maximize the alignment. Lines indicate zinc finger regions. Asterisks (*) indicate cysteine, histidine, leucine, and phenylalanine (or tyrosine) residues conserved in zinc finger sequences. Note that mSNA lacks the key residues of the first zinc finger. (B) Evolutionary tree analysis of SNAIL-related proteins. Homologies among proteins were calculated based on the zinc finger regions. (C) Alignment of the amino termini of several gene products found in the GenBank database. The SNAG domain (indicated in bold) is present in vertebrate SNAIL family proteins as well as in Gfi1, Gsh1, and IA1. Note that invertebrate SNAIL-related proteins do not have the SNAG domain. The GenBank accession numbers for the sequences are rat Gfi1, L06986; mouse Gsh1, U21224; and human IA1, U07172. Other accession numbers are indicated above.

stained with DAPI for analysis by fluorescence-activated cell sorting (FACS). Analysis was also performed on adherent cells: Rcho-1 stem cells that were plated for 48 h and trypsin-resistant giant cells were fixed in methanol and stained with bisbenzimide. Nuclear DNA content was estimated by fluorescence intensity on 50–100 cells for each population using an imaging system from Compix Inc. Imaging Systems (Cranberry Township, PA). Fluorescent intensity was compared to serum-starved, quiescent HeLa cells that were shown to be diploid by FACS analysis.

## RESULTS

***Relationship of mSna to the Drosophila Escargot gene.*** We were interested in the possibility that a mammalian homologue of *Escargot* may regulate the transition to endoreduplication in rodent trophoblast giant cells. The cloning of *mSna* revealed that it was homologous to the Drosophila *Snail* and *Escargot* genes. However, despite its name, *mSna* was found to have greater similarity to *Escargot* in the zinc finger region (Smith *et al.,* 1992). As new members have been more recently identified, we have performed a systematic analysis including these new members. Alignments of the deduced amino acid sequences of the large number of Drosophila and vertebrate *Snail* homologues are shown in Fig. 1A. The 109 residues of the mSNA zinc finger domain share 75.2% similarity with dSNAIL, but 85.3% similarity with dESCARGOT. Likewise, after introducing gaps to maximize matching, the sequence N-terminal to the zinc finger domain of mSNA is only 36.1% similar to dSNAIL, but is 49.7% similar to dESCARGOT. Because of this, we suggest that *mSna* is actually more closely related to Drosophila *Escargot* than *Snail.* This is supported by multialignment/evolutionary tree analysis of all published SNAIL-related proteins (Fig. 1B). Notably, mSNA is more closely related to ESCARGOT than to other vertebrate SNAIL family members sequenced to date. Despite these similarities, there are potentially significant differences between *mSna* and Drosophila *Escargot:* (1) mSNA lacks the first zinc finger (Fig. 1A) and (2) Drosophila ESCARGOT lacks the N-terminal SNAG domain (Grimes *et al.,* 1996) found in all vertebrate SNAIL family members (Fig. 1C).

***mSna is expressed in proliferating but not endoreduplicating trophoblast cells.*** The detailed expression patterns of *mSna* in mesodermal and neural crest-derived structures of the embryo proper have been described previously by others (Nieto *et al.,* 1992; Smith *et al.,* 1992). However, while expression had been previously noted in the ectoplacental cone at around day 7.5, expression in trophoblast of the placenta was not studied in detail at other stages. RNA *in situ* hybridization on serial placental sections from day 8.5 murine conceptuses revealed that *mSna* was expressed in cells at the periphery of the ectoplacental cone, which are trophoblast giant cell precursors. These cells also express the basic helix-loop-helix factor *Mash-2* (Guillemot *et al.,* 1994) (Figs. 2A and 2C, arrowheads). In contrast, *mSna* transcripts were absent or present at much lower levels in the proliferative trophoblast of the chorion, where *Mash-2* is strongly expressed (Figs. 2A and 2C, arrows). *mSna* expression was also not detectable in trophoblast giant cells

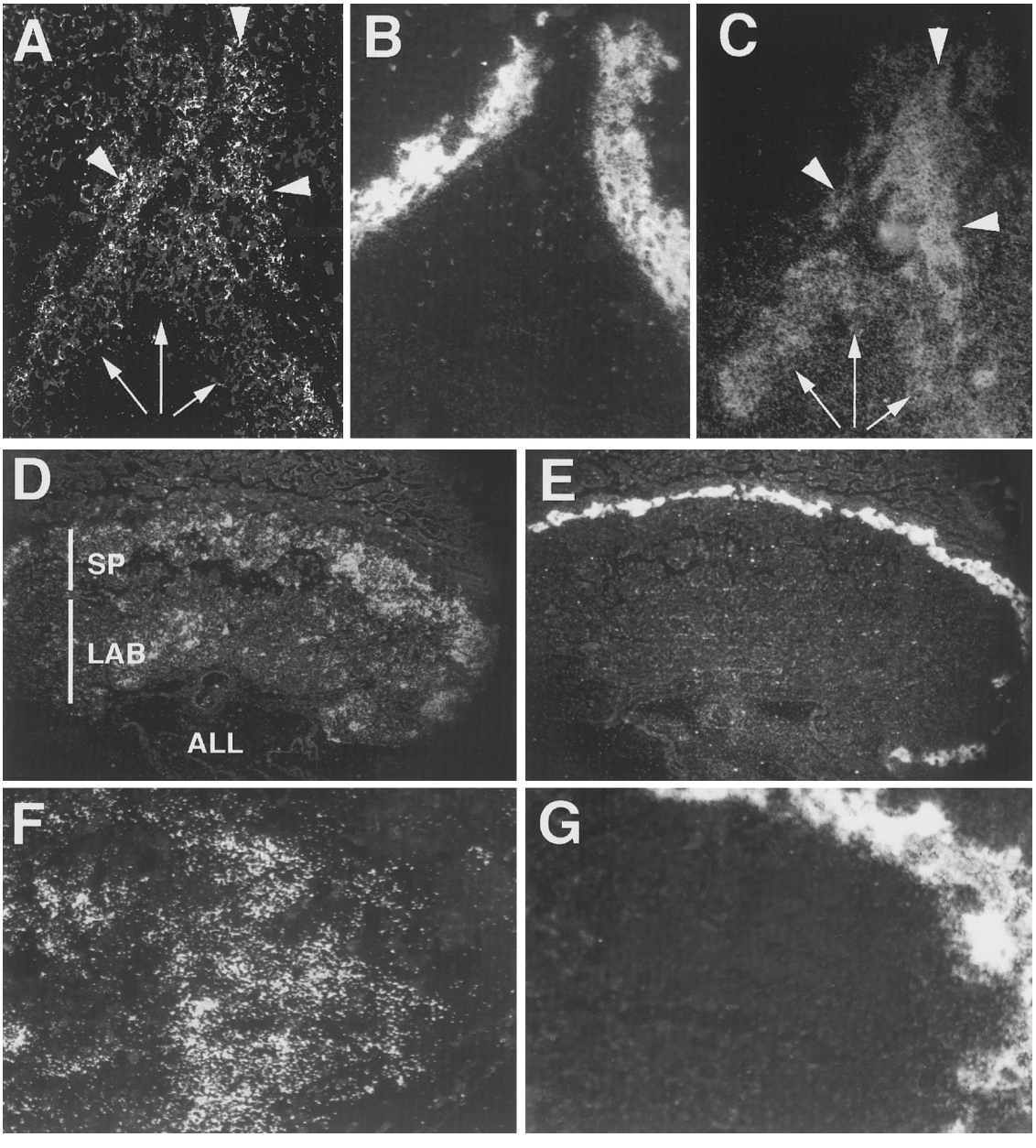


**FIG. 2.** Localization of *mSna* mRNA to trophoblast of the ectoplacental cone and spongiotrophoblast layer, but not to trophoblast giant cells. (A–C) Serial sections of a day 8.5 mouse conceptus hybridized with antisense probes specific to (A) *mSna,* (B) *PL-I,* and (C) *Mash-2. mSna* expression was detectable in trophoblast cells at the periphery of the ectoplacental cone (arrowheads), but not in the chorion (arrows) where *Mash-2* is expressed at high levels. (D–G) Expression of *mSna* (D, F) and *PL-I* (E, G) on adjacent sections of a day 10.5 mouse placenta. *mSna* transcripts are readily detectable in the spongiotrophoblast layer and labyrinth, but not in trophoblast giant cells (indicated by *PL-I* expression). (F, G) High-magnification views of day 10.5 placenta demonstrating lack of *mSna* (F) expression in *PL-I*-positive (G) giant cells. Note nonuniform *mSna* expression in the spongiotrophoblast. ALL, allantois; LAB, labyrinthine layer; SP, spongiotrophoblast layer.

which express the giant cell-specific marker *PL-I* (Shida *et al.,* 1992) (Fig. 2B).

At day 10.5, *mSna* expression was apparent in the spongiotrophoblast layer, which is derived from the ectoplacental cone. However, the signal appeared to be discontinuous in the spongiotrophoblast layer and was restricted to a fraction of the cells (Figs. 2D and 2F), indicating that the spongiotrophoblast layer is heterogeneous in some way. *mSna* expression was also detectable in focal areas of the labyrinthine layer, though we were unable to determine

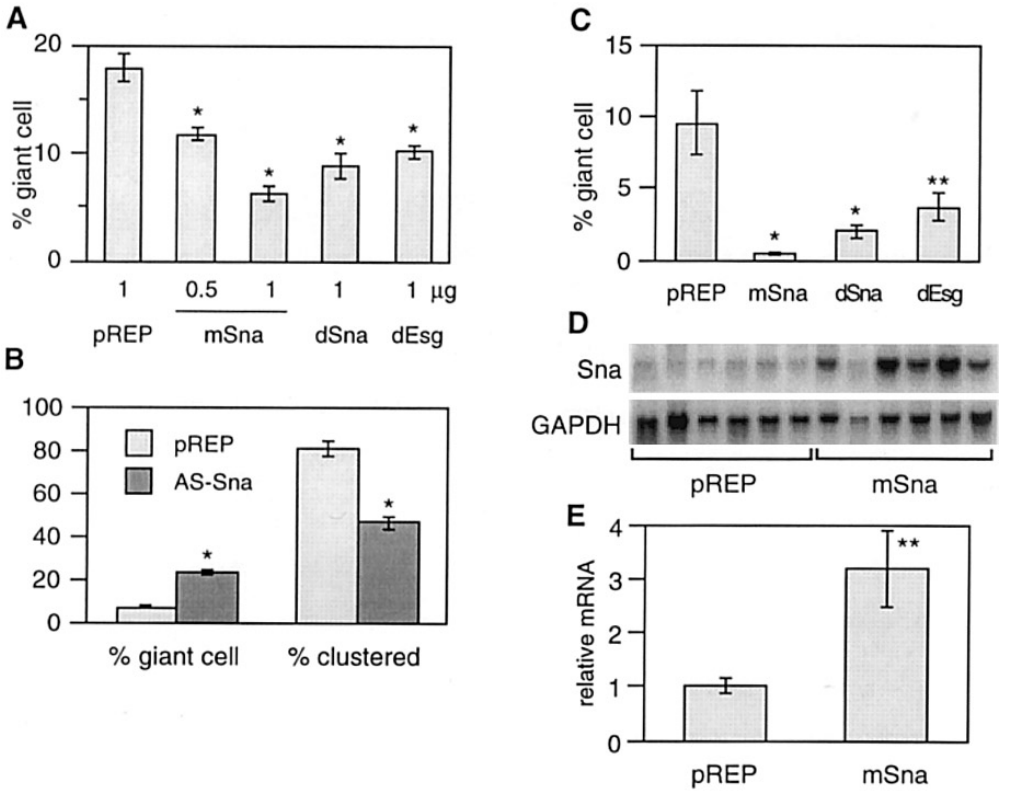


**FIG. 3.** Effect of *mSna* misexpression on giant cell differentiation. (A) Transient expression of *Snail* homologues in Rcho-1 cells. Rcho-1 stem cells were cotransfected with expression vectors encoding *mSna*, *Snail* (*dSna*), and *Escargot* (*dEsg*) or vector alone (control) and pβActin-LacZ at a 5:1 ratio. The proportion of LacZ-positive cells that had differentiated to giant cells was assayed 48 h after transfection. (B) Effect of transient antisense *mSna* expression in Rcho-1 cells. An antisense *mSna* expression vector (AS-Sna) or vector alone (control) was cotransfected with pβActin-LacZ at a 5:1 ratio into Rcho-1 stem cells. The proportion of LacZ-positive cells that had differentiated to giant cells was assayed 60 h after transfection. The percentage of LacZ-positive cells that proliferated to form clusters of cells was also determined. (C) Trophoblast giant cell differentiation in stable Rcho-1 transfectants. Ten independent clones were analyzed for each gene. Trypsin-labile stem cells were plated and the proportion that differentiated to giant cells was counted 48 h later. (D) *Sna* mRNA expression in Rcho-1 stable transfectants. Representative *Sna* and *GAPDH* Northern blots using RNA isolated from control and *mSna*-transfected cells are shown. (E) Quantitation of *Sna* mRNA expression. The *Sna* mRNA levels were normalized to *GAPDH* expression. All graphs (A, B, C, and E) indicate means ± SE and statistically significant differences from control are shown (*$P < 0.01$; **$P < 0.05$).

with this technique if the expression was in the trophoblast- or mesodermally derived component of the labyrinth. Consistent with the findings at day 8.5, *mSna* transcripts were not detectable in trophoblast giant cells. Downregulation of *mSna* expression occurs precisely at the border between populations of spongiotrophoblast and endocycling trophoblast giant cells (Figs. 2D–2G). Placental expression later in development was similar to the patterns at day 10.5 (data not shown). The expression pattern of *mSna* was, therefore, consistent with its putative role in the inhibition of trophoblast giant cell differentiation and/or endoreduplication in the placenta.

***Misexpression of mSna alters the frequency of giant cell differentiation.*** Based on the expression pattern of *mSna*, we wished to determine if *mSna* is capable of regulating the differentiation of trophoblast giant cells. To test this, we transfected a rat trophoblast cell line, Rcho-1 (Faria and Soares, 1991), with expression vectors for *Snail* family members. These cells, which grow as proliferating (stem) cells, spontaneously differentiate at a moderate and reasonably repeatable frequency (typically around 10% within 48 h) to trophoblast giant cells (Cross *et al.*, 1995a). The rate is consistent within experiments but can vary moderately between experiments depending on plating density. Transient expression of *mSna*, as well as Drosophila *Snail* and *Escargot*, significantly decreased the proportion of Rcho-1 stem cells that differentiated to trophoblast giant cells in culture (Fig. 3A). We next produced stable transfectants that expressed significantly elevated amounts of *mSna* mRNA (Figs. 3D and 3E). These cells underwent giant cell differentiation at a markedly (20-fold) reduced level. This antidifferentiation activity was also demonstrated by Drosophila *Snail* and *Escargot* (Fig. 3C). Notably the two Drosophila genes were similarly effective in these assays, although

**TABLE 1**
Cell Cycle Kinetics in *mSna*-Transfected Rcho-1 Cells

| Transfected DNA | Clone | Doubling time[a] | G1[a] | S[a] | G2[a] | M[a] |
|---|---|---|---|---|---|---|
| pREP10 | #1 | 14.6 | 4–5 h | 4.7 h | 4–5 h | 1.0 h |
| | #2 | 13.7 | 4–5 h | 4.3 h | 4–5 h | 0.8 h |
| pREP-mSna | #1 | 14.5 | 4–5 h | 4.2 h | 4–5 h | 0.8 h |
| | #2 | 14.3 | 4–5 h | 4.8 h | 4–5 h | 0.9 h |

[a] Estimates of cell cycle phase lengths were made as described under Materials and Methods.

neither was as potent as *mSna*. To test if endogenous rat *Sna* functions to block differentiation, Rcho-1 *Sna* mRNA levels were lowered via transient transfection of an antisense *mSna* expression vector. Inhibition of *Sna* expression increased the frequency of giant cell differentiation approximately 5-fold (Fig. 3B). Antisense *mSna* transfectants also formed fewer cell clusters after culture at low (clonal) density, suggesting an arrest in cell proliferation (Fig. 3B). Taken together, these data indicate that *mSna* is capable of inhibiting trophoblast giant cell differentiation.

***mSna overexpression does not alter cell cycle kinetics but upregulates cyclin A and B expression.*** Because trophoblast giant cell differentiation is coincident with the switch from the mitotic cell cycle to the endocycle, we tested if *mSna* activity is mediated via alterations of the cell cycle. Estimates of cell cycle parameters, namely cell doubling time and the lengths of cell cycle phases, were made for control and *mSna*-transfected Rcho-1 cells (Table 1). Total cell cycle length in Rcho-1 stem cells was about 14 h. Interestingly, in these rapidly dividing cells, G1 was relatively short. As a result, only 30–40% of cells are in G1 in an unsynchronized population (Fig. 4A; note that Rcho-1 stem cells are tetraploid). Overexpression of *mSna*, *Snail*, and *Escargot* had no significant effects on the cell cycle as detected either by the distribution of DNA contents representative of G1 and G2 phases (Fig. 4B) or by direct estimates of cell cycle phase lengths (Table 1). These data indicated that overexpression of *mSna* had no direct effects

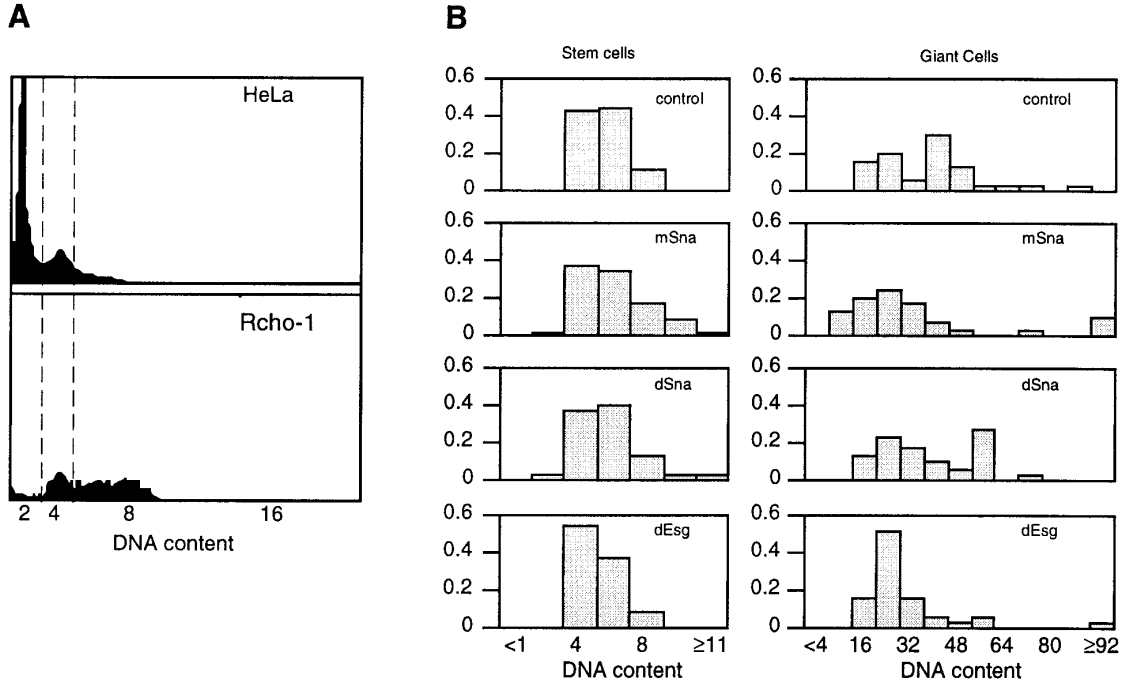


**FIG. 4.** Nuclear DNA content in Rcho-1 cells estimated in cell suspensions by FACS (A) and in adherent cells by scanning fluorometry image analysis (B). For the latter, Rcho-1 stable transfectants for control, *mSna*, *Snail* (*dSna*), and *Escargot* (*dEsg*) were plated on coverslips for 2 days, before fixation and bisbenzimide staining. Nuclear fluorescence intensity was measured for 50–100 cells of each group, including cells with both stem cell and giant cell morphology.

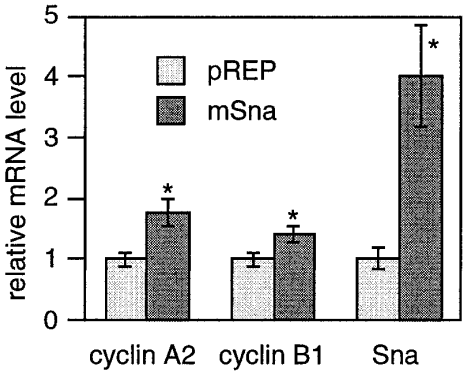


**FIG. 5.** Expression of *cyclin A* and *B* mRNAs in *mSna*-transfected Rcho-1 cells. RNA (10 $\mu$g) from five independent clones of each group were analyzed by Northern blot hybridization and probed for *cyclin A2*, *cyclin B1*, and *Sna*. The hybridization signals are normalized to *GAPDH* expression. * indicates statistically significant difference from control ($P < 0.05$).

on cell cycle parameters in Rcho-1 stem cells. We next tested whether overexpression of *mSna*, *Snail*, and *Escargot* affected DNA synthesis in those few cells that were able to differentiate to giant cells (Fig. 3C). Upon giant cell differentiation, Rcho-1 cells undergo multiple endocycles, with a concomitant rise in DNA content (Fig. 4B). We found that giant cells of all transfectants reached high ploidies, indicating that they could still undergo endoreduplication (Fig. 4B). *mSna* overexpression did not, therefore, affect either the kinetics of the cell cycle or the progression of the endocycle in differentiated trophoblast giant cells, but rather affected the initial transition to the endocycle.

The transition from the mitotic cell cycle to the first endocycle during Rcho-1 cell differentiation occurs during the G2 phase (MacAuley *et al.*, 1998). We therefore tested if overexpression of *mSna* inhibits the cell cycle transition by affecting G2-specific cyclin function. *Cyclin A* and *B* mRNA levels in control and *mSna*-transfected cell lines were measured by Northern blot hybridization. The mRNAs for both cyclins were found to be significantly elevated, even in unsynchronized populations of *mSna* transfectants (Fig. 5). Because of this cell cycle phase-specific effect, we wondered if the expression of *mSna* may itself be cell cycle regulated. Attempts to synchronize Rcho-1 stem cells in G1 using serum starvation or mimosine arrest resulted in giant cell differentiation after release from the blocks (data not shown). Therefore, we measured the expression of *mSna* in NIH/3T3 cells which express the gene and which are easily synchronized. The levels of *mSna* mRNA in synchronized (G1 arrested by serum starvation) NIH/3T3 cells were assessed during cell cycle progression following serum addition. Upon serum addition, *mSna* mRNA levels increased within 1 h, peaked at 3 h, and then fell to intermediate levels that were maintained during cell cycle progression (Figs. 6A and 6B). Therefore, the mRNA levels did not appear to change during the cell cycle. Interestingly, the induction of *mSna* mRNA by serum was not inhibited by the presence of the protein synthesis inhibitor cycloheximide (Fig. 6C), implying that *mSna* is an immediate early response gene.

***mSNA binds to E-box sequences and represses transcription.*** The ability of *Escargot* to repress endoreduplication in *Drosophila* is dependent on the DNA-binding activity of its

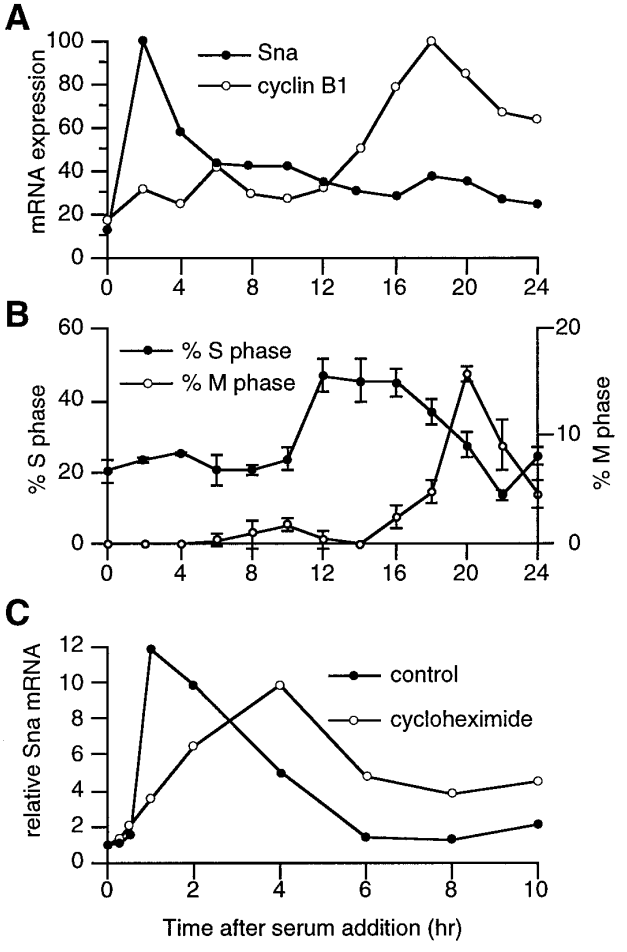


**FIG. 6.** *mSna* mRNA expression during the cell cycle in 3T3 fibroblasts. (A) Changes in *mSna* and *cyclin B1* mRNA in synchronized 3T3 fibroblasts. Cells were synchronized by serum starvation for 3 days and then replated in the presence of serum-containing medium. Relative amounts of mRNAs were assessed by Northern blot hybridization and were normalized to *GAPDH* mRNA levels. (B) Proportion of S- and M-phase cells in a synchronized 3T3 population after serum addition. Cells were pulse labeled with [$^3$H]thymidine at intervals after reintroduction of serum. After autoradiography and counterstaining, the fractions of cells with silver grains and mitotic figures were counted. (C) The effect of protein synthesis inhibitor cycloheximide on *mSna* mRNA induction after serum addition. 3T3 fibroblasts synchronized by serum starvation were released (by serum addition) in the presence or absence of 10 $\mu$g/ml cycloheximide. mRNAs were extracted at 0, 15, and 30 min and 1, 2, 4, 6, 8, and 10 h after release.

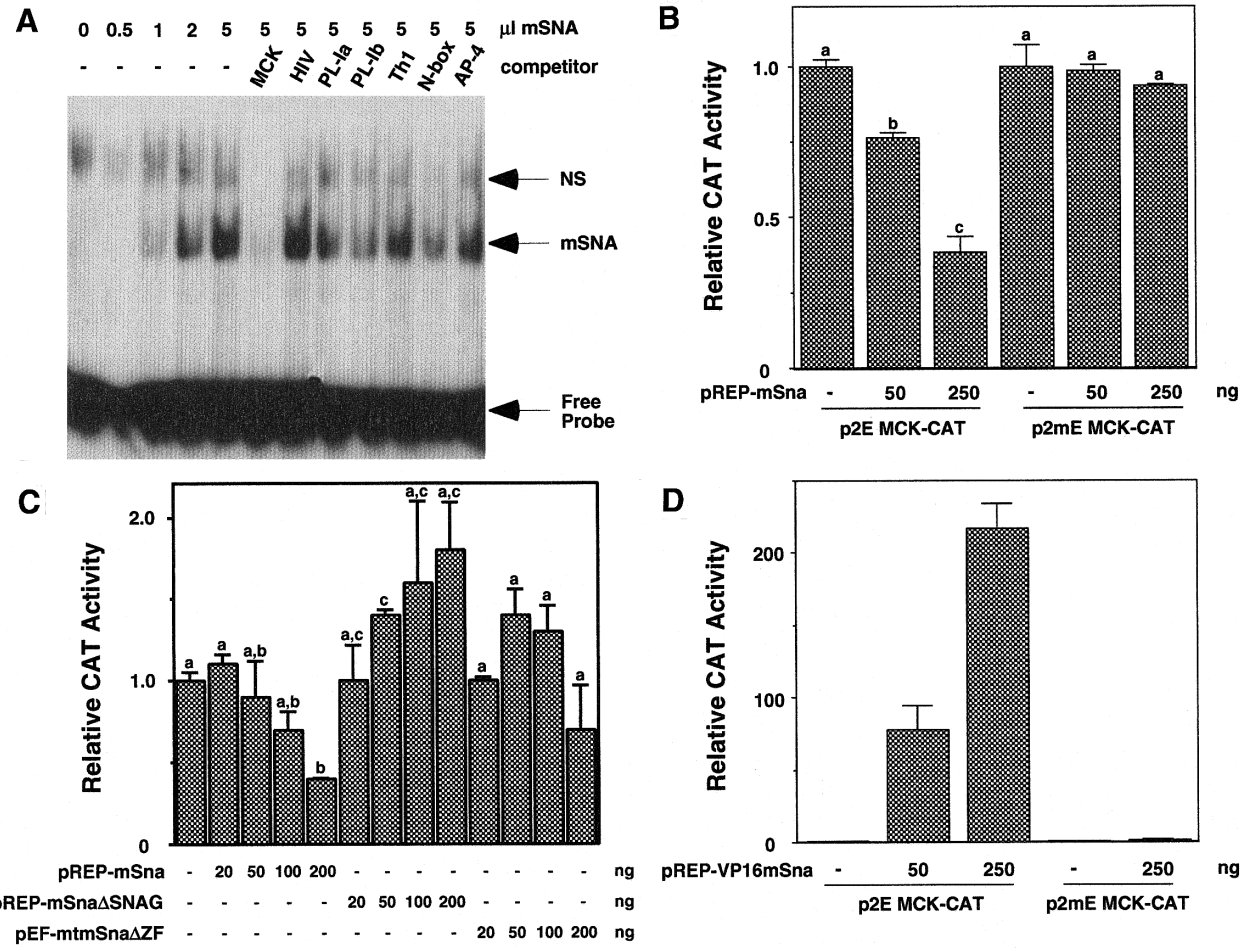


**FIG. 7.** mSNA is a transcriptional repressor that binds to a subset of E-box sequences. (A) Electrophoretic mobility shift assay using a $^{32}$P-labeled MCK E-box probe. The volume of *in vitro* translated mSNA used is indicated; lysate volume was equalized using control (no plasmid) products. The position of the mSNA:E-box complex is indicated by an arrow. For competition assays, a 200-fold excess of the indicated unlabeled sequence was used. NS, nonspecific complex. (B–D) Transcriptional activity of mSNA. Transfection assays in C3H10T1/2 fibroblast cells were carried out using a CAT reporter gene driven by a minimal promoter and two copies of the MCK E-box (p2E MCK-CAT) or two mutated MCK E-boxes (p2mE MCK-CAT). The amount of plasmid used in each transfection was balanced using the pREP7 expression vector. CAT values were normalized to $\beta$-Gal activity due to a cotransfected p$\beta$Actin-LacZ plasmid and are expressed relative to control (pREP7 alone) values (normalized to 1.0). (B) mSNA represses transcription from a promoter containing the MCK E-box but not the mutant, non-E-box sequence. (C) mSNA-mediated transcriptional repression is dependent on both the zinc finger and SNAG domains. (D) A mSNA-VP16 activation domain fusion protein activates transcription. Different superscripts indicate statistically significant differences (ANOVA; $P < 0.05$).

encoded protein, since zinc finger domain mutants that lack DNA-binding activity are unable to rescue the *escargot* phenotype (Fuse *et al.*, 1994). The DNA-binding specificities of SNAIL (Mauhin *et al.*, 1993) and ESCARGOT (Fuse *et al.*, 1994) have been previously studied. *In vitro*, ESCARGOT binds to an E2 box consensus sequence (G/ACAGGTG) as a monomer, where it can act as a transcriptional repressor by antagonizing the binding of basic helix-loop-helix transcription factors such as DAUGHTERLESS and SCUTE (Fuse *et al.*, 1994). In electrophoretic mobility shift assays, mSNA bound to a muscle creatine kinase (MCK) E-box element whose sequence (GCAGGTG) matches the E2 consensus. The relative mobility of the mSNA:DNA complex was consistent with mSNA binding as a monomer (Fig. 7A). mSNA DNA-binding activity appeared to be site specific, as binding to the MCK E-box probe was inhibited by an excess of unlabeled MCK E-box sequences, but incompletely or not at all by a variety of related E-box sequences that do not share the E2 consensus. Therefore, the *in vitro* DNA-binding activity of mSNA was similar to that of ESCARGOT and SNAIL.

To test the transcriptional activity of mSNA, transfection assays were performed in C3H10T1/2 fibroblast cells in

which a chloramphenicol acetyltransferase reporter gene was placed downstream of a promoter and two copies of the MCK E-box sequence. Transfection with an *mSna* expression vector resulted in repression of promoter activity in a concentration-dependent manner (Fig. 7B). mSNA is a member of a zinc finger transcription factor family whose ability to bind DNA resides in its zinc finger motifs (Fuse *et al.*, 1994; Mauhin *et al.*, 1993). Repressor activity was clearly dependent on binding to the MCK E-box sequence, as deletion of the zinc finger domain blocked the ability of mSNA to repress promoter activity (Fig. 7C). Likewise, the activity of a reporter construct bearing two copies of mutated sequence (TACCGTG) was unaffected by *mSna* transfection (Fig. 7B).

Notably, the activity of the mutant reporter construct was similar to that of the promoter bearing wild-type sites demonstrating that the latter had no net enhancer activity in these cells. It is possible that the cells contain a balance of transcriptional activators and repressors that both bind to the same sites, one which is shifted with transfection of *mSna*. Alternatively, mSNA could affect basal transcription directly, if mSNA contains a repressor domain. The amino-terminal seven amino acids of mSNA resemble a SNAG domain, which has been shown to impart transcriptional repressor activity in other contexts (Grimes *et al.*, 1996). A deletion mutant of mSNA lacking the SNAG domain was unable to inhibit basal transcriptional activity from MCK E-boxes (Fig. 7C). In some experiments, transfection with the mutant protein upregulated activity about twofold at high concentrations (Fig. 7C; data not shown). Because C3H10T1/2 cells express *mSna* endogenously (data not shown), the latter effect could be due to competition with the wild-type protein: the mSNAΔSNAG protein could displace the wild-type protein from the binding site. In contrast to the transcriptional repressive effect of mSNA, a fusion protein containing the potent VP16 transcriptional activation domain, in place of the SNAG domain, upregulated transcription up to 200-fold (Fig. 7D); the latter effect was abolished when the E-box sequence was mutated (Fig. 7D). These data suggested that under basal conditions mSNA can act as a transcriptional repressor whose activity is dependent on both binding to E2 box-related sequences (via the zinc finger domain) and an active inhibitory function (mediated by the SNAG domain).

In transfected cells, ESCARGOT can inhibit transcription via competition with helix-loop-helix activators for a common DNA-binding site (Fuse *et al.*, 1994). We explored this model with mSNA using the class A helix-loop-helix proteins E47 and ME2 as well as the cell type-specific protein MASH-2, which are all able to bind to the MCK E-box sequence. In electrophoretic mobility shift assays, the mSNA protein was capable of displacing both E47 homodimer and E47/MASH-2 heterodimer complexes from the MCK E-box in a concentration-dependent fashion (Fig. 8A). Therefore, the binding of mSNA and helix-loop-helix factors to this sequence appeared to be mutually exclusive. Transfection assays were performed in which the MCK

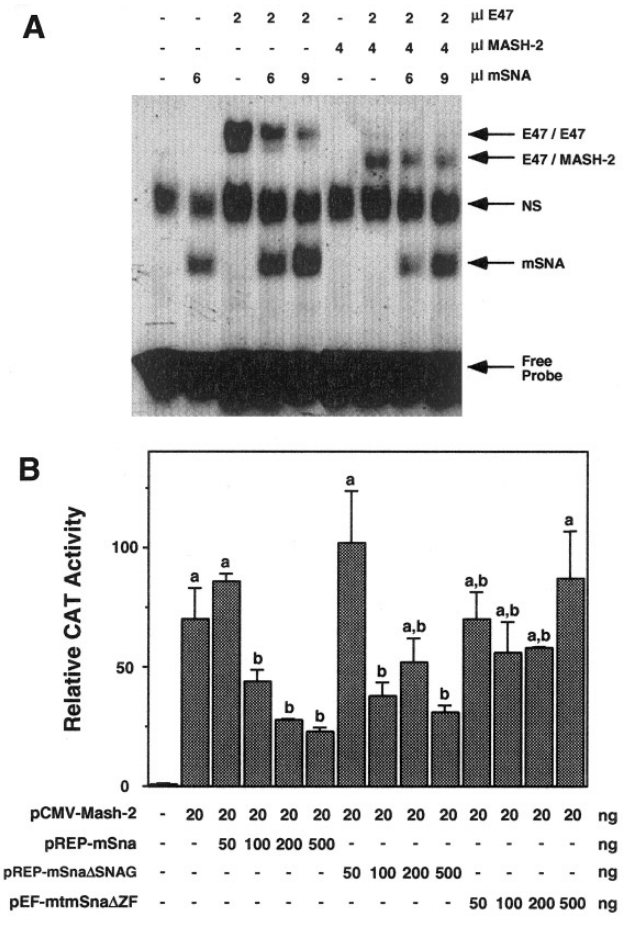


**FIG. 8.** mSNA inhibits basic helix-loop-helix transcription factor activity by competitively binding to the E-box site. (A) Electrophoretic mobility shift assay using a $^{32}$P-labeled MCK E-box probe. The indicated amounts of *in vitro* translated mSNA, E47, and MASH-2 were preincubated prior to the addition of probe, with volumes being equalized using control lysate. The positions of the E47 homodimer, E47/MASH-2 heterodimer, and mSNA monomer complexes with DNA are indicated. NS, nonspecific complex. (B) Transfection assays in C3H10T1/2 fibroblast cells were carried out using the p2E MCK-CAT reporter. Expression vectors encoding full-length, SNAG domain-deleted and zinc finger domain-deleted mSNA were cotransfected with a vector encoding MASH-2. CAT values were normalized to $\beta$-Gal activity due to a cotransfected p$\beta$Actin-LacZ plasmid and are expressed relative to control (pREP7 alone) values (normalized to 1.0). Different superscripts indicate statistically significant differences (ANOVA; $P < 0.05$).

E-box reporter was activated by cotransfection with a *Mash-2* expression vector. Under these conditions, overexpression of *mSna* significantly inhibited *Mash-2*-dependent transcriptional activity in a concentration-dependent manner (Fig. 8B). Interestingly, deletion of the SNAG domain, which blocked the ability of mSNA to inhibit basal transcriptional activity, did not eliminate the inhibitory activity against MASH-2: MASH-2-activated transcription was

significantly reduced by mSNAΔSNAG (Fig. 8B), although perhaps to a slightly lesser degree than mSNA. In contrast, deletion of the zinc finger domain blocked the inhibitory effect (Fig. 8B). Similar results were observed when using ME2 as the activator (data not shown). These data suggested that mSNA can act as a transcriptional repressor by displacement of transactivators from their DNA target sites and that the SNAG domain is not essential for this type of activity. Together the results of the basal and activator-induced transcription assays clearly showed that mSNA can act as a repressor of transcription.

***The zinc finger and SNAG domains are required for the antidifferentiation activity of mSNA.*** As the zinc finger and SNAG domains were required for the transcriptional repressor function of mSNA, we wished to determine if they were also essential for the inhibitory effects of mSNA on Rcho-1 giant cell differentiation. We tested this in transient transfection experiments as described earlier. Deletion of the zinc finger domain abolished the antidifferentiation response to *mSna* overexpression (Fig. 9A). Deletion of the SNAG domain significantly reduced, though did not eliminate, inhibition of giant cell differentiation by *mSna* overexpression. These data strongly suggested that the zinc finger domain is essential for mSNA's antidifferentiation activity, while the SNAG domain is not absolutely required. This finding was consistent with the fact that the Drosophila SNAIL and ESCARGOT proteins, which lack SNAG domains, blocked Rcho-1 cell differentiation as well. We found that addition of an N-terminal myc epitope had no effect on *mSna* function (Fig. 9A). Therefore, we used anti-myc staining to study cellular localization of the mSNA and mSNAΔZF proteins. Both proteins were readily detectable in transfected Rcho-1 stem cells (Fig. 9B), indicating that the loss of antidifferentiation activity of the mSNAΔZF protein was not due to a lack of protein expression. In experiments where transfected cells were identified by virtue of a cotransfected vector encoding the CD20 cell surface marker we found that essentially all transfected cells expressed the mSNA proteins (data not shown). mSNA and mSNAΔZF were localized to both the nucleus and cytoplasm in about 30% of transfected cells, whereas approximately 70% of transfected cells displayed exclusive cytoplasmic staining (Fig. 9B, results not shown).

## DISCUSSION

We have demonstrated here that mSNA is expressed in trophoblast cells of the ectoplacental cone and spongiotrophoblast, which are precursors of giant cells, but is downregulated upon trophoblast giant cell differentiation and moreover that this downregulation is likely essential for differentiation to occur. *In vitro* and in transfection experiments, mSNA acts as a sequence-specific DNA binding protein which represses transcription from promoters containing its binding site. The differentiation-arresting activity of mSNA in trophoblast cells is dependent on the zinc finger DNA-binding domain and, to a lesser extent, on the SNAG domain which has a putative transcriptional repressor effect. We therefore hypothesize that mSNA likely blocks giant cell commitment by repressing the transcription of a gene (or genes) that promotes the transition from the mitotic cell cycle to the first endocycle during trophoblast differentiation.

***mSna has an Escargot-like function.*** In general, the effects of *mSna* reported here resemble the activity of the Drosophila *Escargot* gene as a repressor of endoreduplication. Obviously the complete comparison awaits analysis of *mSna*-deficient mice in order to determine if loss of function results in ectopic or premature endoreduplication. We cannot, at present, rule out the possibility that there are other *Escargot*-related genes in mice. However, at least in trophoblast, we suggest that *mSna* has *Escargot*-like function. First, its expression pattern—downregulation coincident with differentiation into giant cells—fits precisely with a role in blocking the transition to the endocycle in precursor cells. Second, it has similar DNA-binding activity and specificity despite the fact that mSNA has four zinc fingers whereas ESCARGOT has five. The apparently greater similarity in structure between mSNA and ESCARGOT that first caught our attention may in fact be insignificant because in our assays transfections of Drosophila *Snail* and *Escargot* were equally effective in blocking Rcho-1 cell differentiation. As such, the proteins may have similar molecular activity. In support of this suggestion, the phenotype of *escargot/snail* double-mutant Drosophila embryos, which is distinct from the single mutants, can be rescued by overexpression of *Escargot* alone (Fuse *et al.*, 1996).

An obvious difference between mSNA and ESCARGOT function is that none of the Drosophila *Snail*-related family members encode proteins with SNAG domains at their N-termini, whereas all of the vertebrate family members do. We have not explored here the precise function of the SNAG domain. However, others have found that the SNAG domain has transcriptional repressor activity and suggested that it may recruit a corepressor complex to promoters (Grimes *et al.*, 1996). Consistent with this, deletion of the SNAG domain from mSNA in our experiments reduced its transcriptional repressive and antidifferentiation activities in certain contexts. Nonetheless, SNAG domain-deficient mSNA still retained significant activity for both effects, implying that the putative corepressor function may not be essential for mSNA function. Consistent with this, both ESCARGOT and SNAIL (which lack SNAG domains) blocked giant cell differentiation in Rcho-1 cells, though the magnitudes of their effects were less than that observed with mSNA. We tentatively conclude from this that the SNAG domain confers no additional novel activity to mSNA but rather simply enhances the transcriptional repression effect. The repression by mSNA could, therefore, be exerted via two mechanisms. First, after mSNA binding to DNA, the recruitment of a repressor complex to a target gene promoter would actively reduce gene transcription and/or promote long-term silencing. Such an activity would clearly depend on both the DNA-binding and SNAG domains. Second, DNA-binding alone could displace transac-

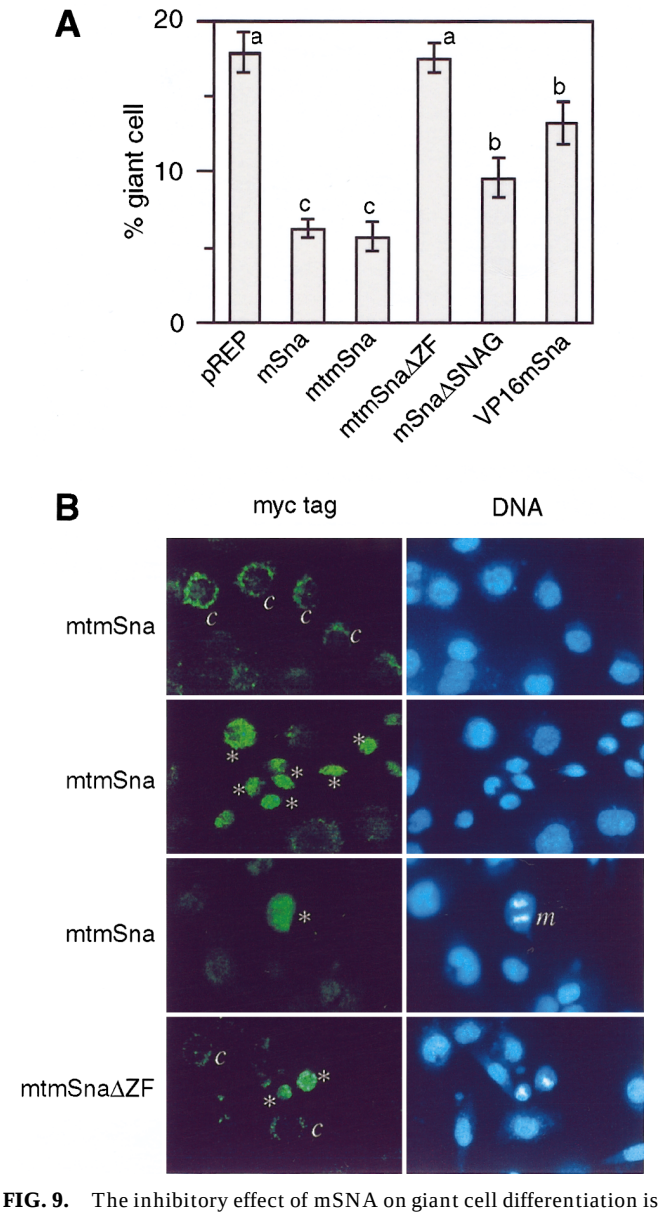


**FIG. 9.** The inhibitory effect of mSNA on giant cell differentiation is dependent on the SNAG and zinc finger domains. (A) Transient transfection of Rcho-1 cells with vectors encoding mSNA, myc epitope-tagged mSNA (mtmSNA), myc epitope-tagged mSNA with a deleted zinc finger domain (mtmSNAΔZF), mSNA lacking the SNAG domain (mSNAΔSNAG), a mSNA-VP16 activation domain fusion (VP16mSNA), or vector alone (pREP). Rcho-1 stem cells were cotransfected with a LacZ expression vector as described in the legend to Fig. 3. The graph indicates the percentage of LacZ-positive cells that differentiated to giant cells (mean ± SE). Superscripts indicate statistically significant differences ($P < 0.05$). (B) Immunolocalization of myc-tagged mSNA fusion proteins in Rcho-1 cells. Vectors encoding full-length (mtmSNA) and zinc finger domain-deleted (mtmSNAΔZF) mSNA were transiently transfected into Rcho-1 cells. The 9E10 anti-c-myc antibody and bisbenzimide staining were used to localize myc-tagged mSNAΔZF (left) and DNA (right). Figures show representative localization patterns. Note that in different cells the proteins localize to either the cytoplasm (*c*) or the nucleus plus cytoplasm (*). In M-phase cells (*m*), the protein is present throughout the cell.

tivators that share the same target sites. Because the SNAIL (Mauhin *et al.*, 1993) and ESCARGOT (Fuse *et al.*, 1994) proteins preferentially bind *in vitro* to E-box elements that resemble binding sites for many helix-loop-helix transcription factors, it was previously suggested that these zinc finger factors could antagonize helix-loop-helix transcription factor function (Fuse *et al.*, 1994). We show here that mSNA is likewise able to bind to specific E-box elements and that indeed this binding is mutually exclusive with that of helix-loop-helix factors.

***Role of mSNA in trophoblast differentiation.*** Although the role of the Drosophila *Snail/Escargot*-related genes during development is well described, the downstream genes that they directly control are less well understood. Genetic evidence suggests, however, that *Snail*-related genes cooperate during *Drosophila* development with helix-loop-helix transcription factors that function as lineage-specific activators of transcription. For example, during neurogenesis the *achaete/scute* helix-loop-helix proteins activate neuronal genes, whereas the *scratch* gene, which encodes a SNAIL-related protein, represses epidermal genes (Roark *et al.*, 1995). Recent evidence suggests an important role for helix-loop-helix transcription factors in controlling trophoblast growth and differentiation. The *Mash-2* gene is essential for maintenance of diploid trophoblast of the mouse spongiotrophoblast layer (Guillemot *et al.*, 1994). *Mash-2* and *mSna* expression overlap in the ectoplacental cone early in development and later in its derivative, the spongiotrophoblast layer. Based on the effects shown here, mSNA can block MASH-2-containing complexes from binding to DNA *in vitro*. Whether mSNA and MASH-2 share common targets *in vivo* is not clear, however. Arguing against this hypothesis, the effect of overexpressing *mSna* in Rcho-1 cells in blocking giant cell differentiation appears similar to that of *Mash-2*. In contrast to *Mash-2*, *Hxt* induces growth arrest, changes in cell adhesiveness, and activation of placental lactogen-I (PL-I) gene expression, features of trophoblast giant cell differentiation (Cross *et al.*, 1995a). Because *Hxt* is expressed not only in giant cells but also in their diploid precursors (in which *Hxt* and *mSna* expressions appear to overlap), its activity could in theory be inhibited until giant cell commitment occurs. Although *Hxt* encodes a helix-loop-helix factor, it is not clear that it binds to E-box sequences (Cross *et al.*, 1995a; Hollenberg *et al.*, 1995). Therefore, an antagonism between HXT and mSNA, while appealing as a model, has no biochemical support at present.

***Cell cycle effects of mSna.*** The transition to the endoreduplication program in trophoblast occurs during the G2 phase of a normal replicative cell cycle, beginning with an arrest of cyclin B activity (MacAuley *et al.*, 1998). Because the effect of altering *mSna* expression levels was in modulating the cell cycle transition phase and not in some more generalized cell cycle effect, it was suspected that *mSna* regulates G2-specific events. Consistent with this hypothesis, *cyclinA* and *B* mRNA levels were significantly elevated in Rcho-1 lines stably overexpressing *mSna*. The

obvious implication from this finding is that maintenance of high cyclin A and B levels in the G2 phase of replicating cells will result in subsequent mitosis, whereas, if the levels are reduced, mitosis will not occur and endocycling can begin. Our findings on the effect of *mSna* are similar to observations made from Drosophila *escargot* mutants, where cyclin A expression is no longer maintained in cells that go on to endoreduplicate (Hayashi, 1996). The model could account for why in endoreduplicating cells a new round of DNA synthesis is not blocked even though this normally does not occur until completion of mitosis: at least one of the inhibitory mechanism in fission yeast depends on cyclin B/cdk1 (Hayles *et al.*, 1994), an activity that is downregulated at giant cell commitment.

By *in situ* hybridization, we found that *mSna* mRNA was expressed nonuniformly in the spongiotrophoblast layer, indicating some heterogeneity in cell phenotype that has not been observed for other genes such as *Hxt* or *4311* (I. C. Scott, unpublished observations). The expression of *Mash-2* is also heterogeneous within the spongiotrophoblast layer at midgestation (Nakayama *et al.*, 1997), but on serial histological sections the *Mash-2* and *mSna* expressing and nonexpressing domains did not appear to correspond. Given the cell cycle phase-specific function and the heterogeneous mRNA expression levels *in vivo*, we wondered initially whether *mSna* itself was cell cycle regulated, but this did not appear to be the case. However, it was impossible to test this clearly in trophoblast cells because all the treatments that we used on the replicating Rcho-1 stem cells, to arrest and therefore synchronize them, promoted giant cell differentiation. Using synchronized 3T3 cells, which also express the gene, we clearly found that *mSna* mRNA levels do not vary during the cell cycle. Nonetheless, *mSna* mRNA expression was serum responsive, and the rapid induction of *mSna* occurred even in the presence of the protein synthesis inhibitor cycloheximide. These data indicate that *mSna* is a serum-inducible, immediate early gene. Therefore, the heterogeneous expression of *mSna* in the spongiotrophoblast layer may reflect cells under varying degrees of growth factor stimulation. Although the mRNA was not cell cycle regulated, we cannot currently exclude the possibility that the mSNA protein may be regulated. In experiments in which we transfected cells with epitope-tagged mSNA, we found that the protein was not uniformly localized in cells. In only 30% of cells was the protein localized to the nucleus (as well as the cytoplasm). The nuclear localization was expected given that the protein appears to function as a DNA-binding transcription factor. However, the protein appeared to be excluded from the nucleus in 70% of cells, in which it was detected solely in the cytoplasm. Although we cannot rule out the possibility that this result was due to overexpression, it will be of interest to know if the endogenous protein shows this similar variation in intracellular localization and, if so, whether it is related to cell cycle events.

In conclusion, mSNA appears to function, in the trophoblast cell lineage at least, as a regulator of the transition in cell cycle structure that occurs during the terminal stages of differentiation. The loss of its expression may allow the transition in cell cycle structure to occur which results in endoreduplication. The target genes directly regulated by mSNA which affect this transition are unknown. However, we do not favor the hypothesis that the mSNA targets are specific to the process of endoreduplication per se since *mSna*, like *Escargot*, is expressed in other cell types that are not believed to endoreduplicate as a normal part of development (e.g., mesoderm). Therefore, if the genes regulated by mSNA are common to multiple cell types, it seems more likely that mSNA is a general regulator of cell cycle progression. The immediate early response gene properties of *mSna* are consistent with this hypothesis. Alternatively, it is possible that mSNA does not regulate cell cycle events directly but rather simply regulates genes which modulate cell differentiation pathways. In some lineages, such as in trophoblast, this differentiation program may be intimately tied secondarily to cell cycle changes, whereas in others the latter may not occur. The identification of mSNA-regulated genes will help resolve this issue.

## ACKNOWLEDGMENTS

The authors thank T. Gridley, S. Hayashi, and D. Linzer for plasmids, T. Davies for discussions and comments on the manuscript, and L. Borzel for editorial assistance. This work was supported by a grant from the Medical Research Council (to J.C.C.). I.C.S. is supported by a studentship from the Natural Science and Engineering Research Council and J.C.C. is a Scholar of the Medical Research Council.

## REFERENCES

Amon, A., Tyers, M., Futcher, B., and Nasmyth, K. (1993). Mechanisms that help the yeast cell cycle clock tick: G2 cyclins transcriptionally activate G2 cyclins and repress G1 cyclins. *Cell* **74,** 993–1007.

Blanar, M. A., and Rutter, W. J. (1992). Interaction cloning: Identification of a helix-loop-helix zipper protein that interacts with c-Fos. *Science* **256,** 1014–1018.

Chapman, D. L., and Wolgemuth, D. J. (1992). Identification of a mouse B-type cyclin which exhibits developmentally regulated expression in the germline. *Mol. Reprod. Dev.* **33,** 259–269.

Chiaramello, A., Soosaar, A., Neuman, T., and Zuber, M. X. (1995). Differential expression and distinct DNA-binding specificity of ME1a and ME2 suggest a unique role during differentiation and neuronal plasticity. *Brain Res. Mol. Brain Res.* **29,** 107–118.

Cross, J. C., Flannery, M. L., Blanar, M. A., Steingrimsson, E., Jenkins, N. A., Copeland, N. G., Rutter, W. J., and Werb, Z. (1995a). Hxt encodes a basic helix-loop-helix transcription factor that regulates trophoblast cell development. *Development* **121,** 2513–2523.

Cross, S. M., Sanchez, C. A., Morgan, C. A., Schimke, M. K., Ramel, S., Idzerda, R. L., Raskind, W. H., and Reid, B. J. (1995b). A p-53 dependent mouse spindle checkpoint. *Science* **267,** 1353–1356.

Evan, G. I., Lewis, G. K., Ramsay, G., and Bishop, J. M. (1985). Isolation of monoclonal antibodies specific for human c-*myc* proto-oncogene product. *Mol. Cell. Biol.* **5,** 3610–3616.

Faria, T. N., and Soares, M. J. (1991). Trophoblast cell differentiation: Establishment, characterization, and modulation of a rat trophoblast cell line expression members of the placental prolactin family. *Endocrinology* **129,** 2895–2906.

Fort, P., Marty, L., Piechaczyk, M., el Sabrouty, S., Dani, C., Jeanteur, P., and Blanchard, J. M. (1985). Various rat adult tissues express only one major mRNA species from the glyceraldehyde-3-phosphate-dehydrogenase multigenic family. *Nucleic Acids Res.* **13,** 1431–1442.

Fuse, N., Hirose, S., and Hayashi, S. (1994). Diploidy of Drosophila imaginal cells is maintained by a transcriptional repressor encoded by escargot. *Genes Dev.* **8,** 2270–2281.

Fuse, N., Hirose, S., and Hayashi, S. (1996). Determination of wing cell fate by the *escargot* and *snail* genes in *Drosophila. Development* **122,** 1059–1067.

Grimes, H. L., Chan, T. O., Zweidler-McKay, P. A., Tong, B., and Tsichlis, P. N. (1996). The Gfi-1 proto-oncoprotein contains a novel transcriptional repressor domain, SNAG, and inhibits $G_1$ arrest induced by interleukin-2 withdrawal. *Mol. Cell. Biol.* **16,** 6263–6272.

Guadagno, T. M., and Newport, J. W. (1996). Cdk2 kinase is required for entry into mitosis as a positive regulator of cdc2-cylcin B kinase activity. *Cell* **84,** 73–82.

Guillemot, F., Nagy, A., Auerbach, A., Rossant, J., and Joyner, A. L. (1994). Essential role of Mash-2 in extraembryonic development. *Nature* **371,** 333–336.

Hartwell, L. H., and Kastan, M. B. (1994). Cell cycle control and cancer. *Science* **266,** 1821–1828.

Hayashi, S. (1996). A Cdc2 dependent checkpoint maintains diploidy in *Drosophila. Development* **122,** 1051–1058.

Hayashi, S., Hirose, S., Metcalfe, T., and Shirras, A. D. (1993). Control of imaginal cell development by the *escargot* gene of *Drosophila. Development* **118,** 105–115.

Hayles, J., Fisher, D., Wollard, A., and Nurse, P. (1994). Temporal order of S phase and mitosis in fission yeast is determined by the state of the $p34^{cdc2}$–mitotic B cyclin complex. *Cell* **78,** 813–822.

Hollenberg, S. M., Sternglanz, R., Cheng, P. F., and Weintraub, H. (1995). Identification of a new family of tissue-specific basic helix-loop- helix proteins with a two-hybrid system. *Mol. Cell. Biol.* **15,** 3813–3822.

Jackson, L. L., Colosi, P., Talamantes, F., and Linzer, D. I. (1986). Molecular cloning of mouse placental lactogen cDNA. *Proc. Natl. Acad. Sci. USA* **83,** 8496–8500.

Johnson, J. E., Birren, S. J., and Anderson, D. J. (1990). Two rat homologues of Drosophila achaete–scute specifically expressed in neuronal precursors. *Nature* **346,** 858–861.

Johnson, J. E., Birren, S. J., Saito, T., and Anderson, D. J. (1992). DNA binding and transcriptional regulatory activity of mammalian achaete–scute homologous (MASH) proteins revealed by interaction with a muscle-specific enhancer. *Proc. Natl. Acad. Sci. USA* **89,** 3596–3600.

MacAuley, A., Cross, J. C., and Werb, Z. (1998). Reprogramming the mammalian cell cycle for endoreduplication in rodent trophoblast cells. *Mol. Biol. Cell* **9,** 795–807.

Marais, R., Light, Y., Paterson, H. F., and Marshall, C. J. (1995). Ras recruits Raf-1 to the plasma membrane for activation by tyrosine phosphorylation. *EMBO J.* **14,** 3136–3145.

Mauhin, V., Lutz, Y., Dennefeld, C., and Alberga, A. (1993). Definition of the DNA-binding site repertoire for the *Drosophila* transcription factor SNAIL. *Nucleic Acids Res.* **21,** 3951–3957.

Millen, K., and Hui, C. (1996). Radioactive hybridization of tissue sections. *In* ''A Laboratory Guide to RNA: Isolation, Analysis and Synthesis'' (P. Krieg, Ed.), pp. 339–355. Wiley-Liss, New York.

Nakayama, H., Liu, Y., Stifani, S., and Cross, J. C. (1997). Developmental restriction of *Mash-2* expression in trophoblast correlates with potential activation of the NOTCH-2 pathway. *Dev. Genet.* **21,** 21–30.

Ng, Y. K., George, K. M., Engel, J. D., and Linzer, D. I. (1994). GATA factor activity is required for the trophoblast-specific transcriptional regulation of the mouse placental lactogen I gene. *Development* **120,** 3257–3266.

Nieto, M. A., Bennett, M. F., Sargent, M. G., and Wilkinson, D. G. (1992). Cloning and developmental expression of *Sna,* a murine homologue of the *Drosophila snail* gene. *Development* **116,** 227–237.

Riley, P., Anson-Cartwright, L., and Cross, J. C. (1998). The Hand1 helix-loop-helix transcription factor is essential for placentation and cardiac morphogenesis. *Nature Genet.* **18,** 271–275.

Roark, M., Sturtevant, M. A., Emery, J., Vaessin, H., Grell, E., and Bier, E. (1995). scratch, a pan-neural gene encoding a zinc finger protein related to snail, promotes neuronal development. *Genes Dev.* **9,** 2384–2398.

Sambrook, J., Fritsch, E. F., and Maniatis, T. (1989). ''Molecular Cloning: A Laboratory Manual,'' 2nd ed. Cold Spring Harbor Laboratory Press, Cold Spring Harbor, NY.

Sherr, C. J. (1993). Mammalian $G_1$ cyclins. *Cell* **73,** 1059–1065.

Shida, M. M., Jackson-Grusby, L. L., Ross, S. R., and Linzer, D. I. (1992). Placental-specific expression from the mouse placental lactogen II gene promoter. *Proc. Natl. Acad. Sci. USA* **89,** 3864–3868.

Smith, D. E., Del Amo, F. F., and Gridley, T. (1992). Isolation of *Sna,* a mouse gene homologous to the *Drosophila* genes *snail* and *escargot:* Its expression pattern suggests multiple roles during postimplantation development. *Development* **116,** 1033–1039.

Sweeney, C., Murphy, M., Kubella, M., Ravnik, S. E., Hawkins, C. F., Wolgemuth, D. J., and Carrington, M. (1996). A distinct cyclin A is expressed in germ cells in the mouse. *Development* **122,** 53–64.

Varmuza, S., Prideaux, V., Kothary, R., and Rossant, J. (1988). Polytene chromosomes in mouse trophoblast giant cells. *Development* **102,** 127–134.

Zybina, E. V., and Zybina, T. G. (1985). Polyteny and endomitosis in supergiant trophoblast cells of the gray vole *Microtus subarvalis. Tsitologiia* **27,** 402–410.

Received for publication October 22, 1997
Accepted March 31, 1998